J. Serb. Chem. Soc. 71 (11) 1237–1246 (2006)
JSCS–3516

UDC 661.183.8.004.12:535.42:66:023
Original scientific paper

The sorption and crystallographic characteristics of alumina activated in a reactor for pneumatic transport

LJILJANA ROŽIĆ[1*#], TATJANA NOVAKOVIĆ[1#], SRĐAN PETROVIĆ[1#], ŽELJKO ČUPIĆ[1#], ŽELJKO GRBAVČIĆ[2] and ALEKSANDAR ROSIĆ[3]

[1]*ICTM-Department of Catalysis and Chemical Engineering, Njegoševa 12, Belgrade, Serbia,* [2]*Faculty of Technology and Metallurgy, University of Belgrade, Karnegijeva 4, Belgrade and* [3]*Faculty of Mining and Geology, University of Belgrade, Đušina 7, Belgrade (e-mail: ljrozic@nanosys.ihtm.bg.ac.yu)*

(Received 20 October 2005, revised 3 March 2006)

Abstract: Active transition alumina powders were obtained by flash calcination of gibbsite in a reactor for pneumatic transport in the dilute, two-phase flow regime in the temperature interval from 883 to 943 K with a residence time between 0.4 and 0.9 s. The results of X-ray diffraction analysis confirmed that the activated alumina samples were either microcrystalline or amorphous. From nitrogen adsorption–desorption isotherms, the specific surface areas of all samples were calculated by the BET method. Using the sorption data, the fractal dimension of the surface of the alumina samples was calculated according to a modified FHH method. By application of fractal geometry, using the values of the fractal dimension of the surface and of the specific surface area, the effective surface areas of the active aluminas were calculated for the adsorption of molecules having a cross-section area greater than that of the nitrogen molecule

Keywords: pneumatic transport, transition amorphous aluminas, X-ray diffraction, fractal dimension.

INTRODUCTION

Transition aluminas obtained from gibbsite by flash calcination are commonly used for the production of catalyst carriers and adsorbents. On heating gibbsite at 673–1073 K for less than 1 s, quasi-amorphous products with the general composition $Al_2O_3 \cdot xH_2O$ (where $0.2 \leq x \leq 1$) are obtained. The transition aluminas obtained in this way are fundamentally different from the producs obtained by gradual calcination of gibbsite. They are highly defective, have increased surface energy and exhibit higher chemical reactivity.[1–3] Several methods for the implementation of the thermal decomposition process have been developed: thermal decom-

* Corespoding author.

\# Serbian Chemical Society active member.

doi: 10.2298/JSC0611237R

position in flue gas backflow at high temperatures, thermal decomposition in flue gas backflow at moderate temperature and a certain pressure of steam, thermal decomposition in fluidized beds of a catalyst or solid heat carrier and thermal decomposition in a thin bed in flowing flue gases.[4–6]

Studies of the effect of temperature on the degree and kinetics of gibbsite dehydration as well as on its phase transformations, described in a previous paper,[7] showed that the degree of dehydration of gibbsite in a reactor for pneumatic transport in the dilute two phase flow regime, with a residence time of 0.4–0.9 s in the heated zone and amorphization of the obtained activated alumina powder increased with increasing temperature in the range from 883 to 943 K. As a consequence of the partial dehydration of gibbsite, open micro- and mesopores isnside the grains of the original gibbsite crystals were formed. The pores in these materials were very often different from the idealized, smooth cylinders, which are usually assumed to exist when modeling porous media. Theoretical and computer simulation studies have shown that the degree of roughness of the pore surfaces strongly influences the rate of mass transfer down the pores.[8] Hence, it is important to be able to quantify the degree of surface structural heterogeneity in transition aluminas.[9] The concept of fractals may offer a method by which apparently irregular surfaces may be both characterized and mathematically modeled. The fractal sets are infinitely fragmented or rough mathematical objects which have detail on all scales. They are characterized by fractal dimensions which give information about the morphology of a set and, more particularly, about their space filling capacity. The value of the fractal dimension of a surface (D_f) can vary from 2, for a perfectly smooth surface to 3, for a very rough surface.

Analysis of a single isotherm using a modified Frenkel–Halsey–Hill (FHH) theory[10] allows the determination of the fractal dimension of a surface. It was found that the use of this theory is limited by the number of adsorbed layers on the surface of an adsorbent. The adsorption isotherm shows two different linear regions for rough surfaces but more than two linear regions for smooth surfaces. In the early stages of adsorption (low p/p_0), the effect of surface tension is negligible and the interaction between an adsorbed molecule and the surface of an adsorbent is mainly due to van der Waals forces. However, surface tension (or capillary condensation) effects become more pronounced later on. Hence, an iteration procedure is necessary to enable an appropriate choice of the fractal region of the isotherm.

By applying fractal geometry, the effective surface areas of active alumina for the adsorption of molecules having a cross-section area greater than that of the nitrogen molecule can be calculated,[11] which is of great importance for the application of transition active aluminas in adsorption and catalaytic processes.

The crystallographic structure of an alumina largely determines the properties of its surface.[12] X-Ray powder diffractions (XRPD) can give valuable information about the crystal structure of a material. For example, the crystallite size, the num-

ber of dislocations, the interlayer distance and many other parameters of the lattice can be determined. In this work, it was not intended to obtain exact information on atomic parameters, as the main interest lay in pseudomorphosis relations and the principal features of the defect structure of the aluminas.

The results of studies on the effect of thermal treatment of gibbsite in a reactor for pneumatic transport on the crystallographic characteristics and porous structure of the obtained activated alumina samples are presented in this paper.

EXPERIMENTAL

Gibbsite, obtained as an intermediate in the production of alumina according to the Bayer process (Birač, Zvornik), was used as the starting material for the preparation of active alumina. The experiments were performed using two gibbsite samples with different particles size distributions. The first sample was gibbsite produced on an industrial scale (sample G_0). The second sample was obtained by grinding the industrial gibbsite in a planetary ball mill (sample G). The particle size distribution of the two samples was determined using standard sieves and a Multisizer 3 Coulter Counter.

The thermal treatment of gibbsite was carried out in a specially designed pilot scale reactor for pneumatic transport of gibbsite powder. The gibbsite was introduced into the reaction section using a vibrating feeding device and a pneumatic transport line with an air flowrate of 1 m^3/h. Before commencement of an experiment, the air flow was preheated up to the selected reaction temperature, adjusted by a temperature inlet controller. Four thermocouples situated at the center of the reactor allowed the desired temperature profile to be achieved within the decomposition zone of aluminum oxide trihydrate decomposition. The gibbsite attained the predetermined temperature, from 883 to 943 K, within a residence time in the heated zone of 0.4 to 0.9 s. A cold air flow was used for cooling the outlet mixture of air and activated gibbsite. The amorphous transition aluminas obtained in the pilot scale reactor for pneumatic transport at the optimal residence time of 0.73 s are denoted as PA1, PA2, PA3 and PA4 for activation temperatures of 883, 903, 923 and 943 K, respectively.

The water content of the gibbsite and activated alumina samples was determined by thermogravimetry. The maximum calcinations temperature was 1373 K.

X-Ray diffraction analysis (XRD) was performed on a Philips PW 1710 diffractometer, using, CuK_α radiation. The interlayer distance (d_{hkl}) and the number of dislocations were calculated according to the method described by Klug and Alexander.[13]

Nitrogen adsorption–desorption isotherms of the starting gibbsite and the activated alumina samples were determined at 77 K, using a laboratory high vacuum volumetric apparatus. The samples had previously been outgassed at a pressure of 10^{-3} Pa for 4 h, the starting gibbsite at 383 K, and the thermally activated samples at 523 K. The specific surface areas of the samples, S_{BET}, were determined by the BET method from nitrogen adsorption isotherms up to $p/p_0 = 0.3$.[14–16] The cumulative pore volumes and the pore size distribution, *i.e.,* the diameter of the pores, were calculated from the desorption isotherm branch by the procedure given by Lippens *et al.*[15]

The fractal dimensions of a surface were obtained using the Frenkel–Halsey–Hill equation.[10] The fractal dimension of the surface and the specific surface area were used to calculate the effective surfaces for the adsorption of molecules of known molecular cross-section areas. The values for the molecular cross-section area of the adsorbates (σ), using literature experimental data,[11] were as follows: methane (0.194 nm^2), ethane (0.259 nm^2), benzene (0.352 nm^2), *n*-butane (0.421 nm^2), naphthalene (0.529 nm^2), anthracene (0.707 nm^2), *n*-$C_{22}H_{46}$ (1.26 nm^2), *n*-$C_{28}H_{58}$ (1.57 nm^2) and *n*-$C_{32}H_{66}$ (1.78 nm^2).

RESULTS AND DISCUSSION

The most important parameters affecting the sorption and crystal characteristics of activated alumina synthesized by flash calcination are the particle size of the

starting material and the residence time and temperature of calcination. In order to study the combined effect of these factors on the characteristics of the obtained activated alumina products, experiments were performed with different combinations of these physical parameters.

The particle size distributions of the two starting gibbsite samples are given in Fig. 1.

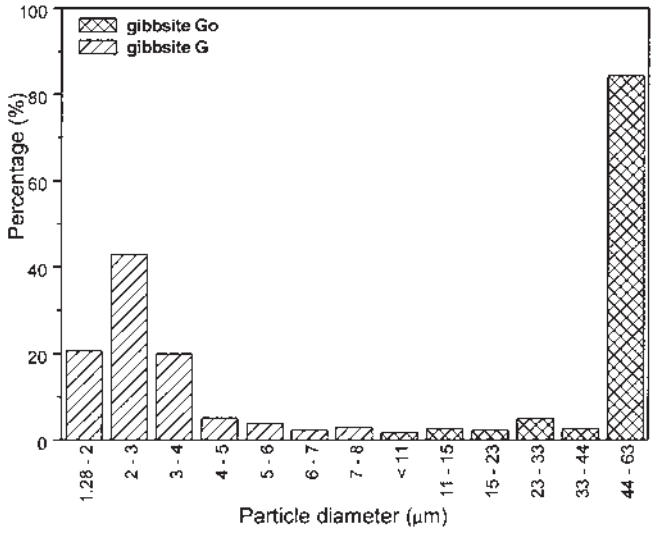

Fig. 1. Particle size distribution of gibbsite produced on an industrial scale (sample G_0) and milled industrial gibbsite (sample G).

The first sample was gibbsite produced on an industrial scale (sample G_0). The second sample was obtained by grinding the industrial gibbsite in a planetary ball mill (sample G).

Particle size analysis of the industrial gibbsite, G_0, revealed that nearly 85 % of the particles had diameters between 40 and 60 μm. The ground sample G, was composed of very fine particles (< 5 μm) with 50 % of the particles having a diameter less than 2.66 μm.

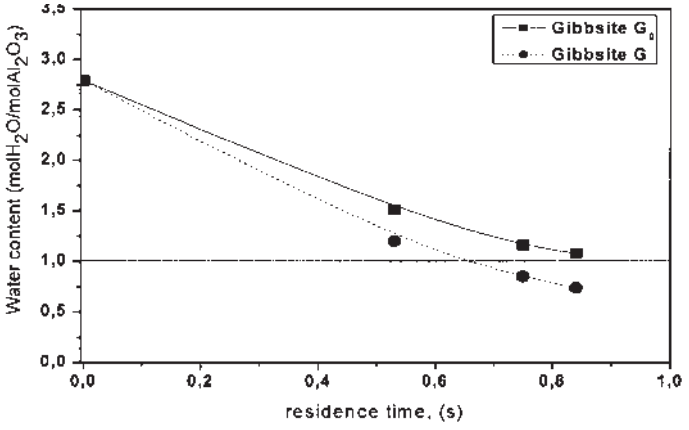

Fig. 2. Dependence of the water content of the activated alumina samples, obtained from industrial gibbsite (G_0) and milled gibbsite (G), on the residence time.

Fine particle sizes are important for the prevention of agglomeration and crystallization of the activated alumina. Under the selected conditions (temperature 923 K, residence time in the heated zone between 0.4 and 0.9 s), the gibbsite samples were partially dehydrated and the residual crystalline water content in the activated products was lower than 1.5 mol H_2O/mol Al_2O_3 (Fig. 2).

After activation, the water content of sample G was lower by about 0.4 mol H_2O/mol Al_2O_3, at the tested residence time, than that of sample G_0. With a residence time equal to or longer than 0.73 s, the water content of sample G was very close to that of alumina monohydrate (horizontal line in Fig. 2).

XRD Powder diffractograms of the activated transition aluminas obtained in the pilot scale reactor for pneumatic transport at a constant residence time of 0.73 s within the temperature range 883–943 K are shown in Fig. 3.

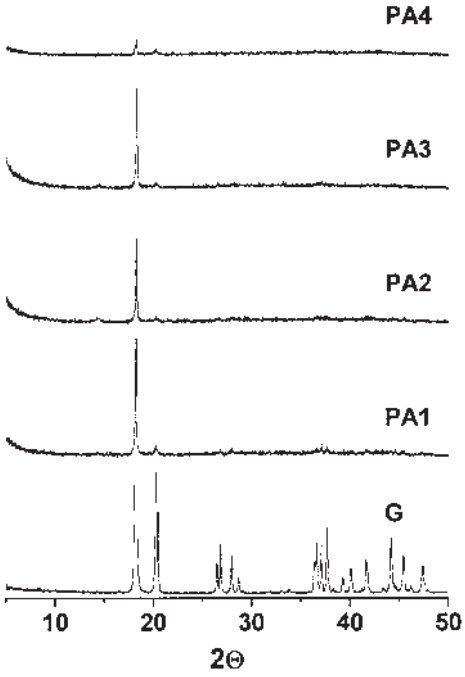

Fig. 3. XRD Patterns of the gibbsite (G) and activated alumina samples (PA1–PA4).

For all the activated samples, only two major diffraction peaks of crystalline gibbsite, located at 2θ values of 18.31° and 20.28°, were visible. The intensity of the gibbsite diffraction lines decreased with increasing temperature and a slight change in other reflections also occurred, indicating that the aluminum oxide was either microcrystalline or amorphous. No recrystallization of the gibbsite into new phases occurred, which means that the activated alumina remained monoclinic-prismatic with the space group P21/n over the entire employed temperature range.

The calculated crystallite size and the number of dislocation[13] for the reflection (110) and (002) for all the activated samples (PA1–PA4) relative to gibbsite (G) are listed in Table I.

TABLE I. Crystallographic data for the reflections (002) and (110) of the starting gibbsite and the activated alumina samples; D-mean crystallite size; ρ-number of dislocation per unit area (cm^2)

Sample	T/K	$D_{(002)}/10^{-5}$ cm	$\rho_{(002)} \cdot 10^{10}$	$D_{(110)}/10^{-5}$ cm	$\rho_{(110)} \cdot 10^{10}$
G	383	–	–	–	–
PA1	883	1.40	1.57	3.20	29
PA2	903	1.40	1.57	0.74	5.5
PA3	923	0.80	4.69	0.74	5.5
PA4	943	0.96	3.25	0.74	5.5

The results show that, in general, there was a slight decrease in the crystallite size of the alumina and a slight increase in the number of dislocation with increasing temperature, but the values remained within the same order of magnitude. The values listed in Table I are meant to be used for relative comparison only.

The activated alumina samples showed a slight linear thermal expansion in the studied temperature range. The values of the lattice interlayer distances, d_{002} and d_{110}, evaluated at each temperature are given in Fig. 4.

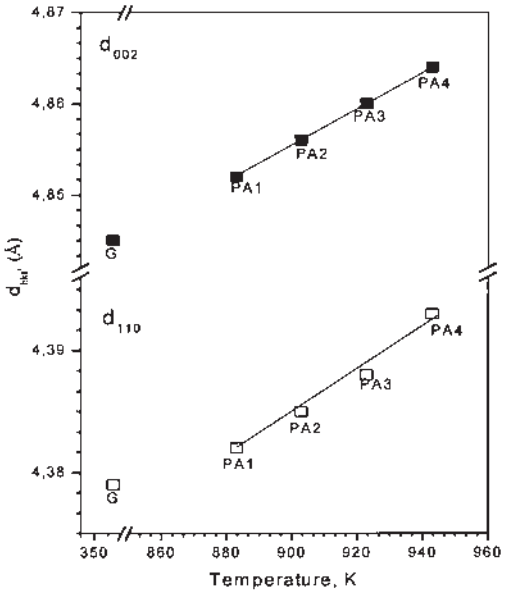

Fig. 4. d-Values derived from the XRD patterns of aluminas activated in the temperature region 883–943 K for the reflection (002) and (110).

The calculated values of d_{002} and d_{110} for all the activated aluminas are slightly larger than those of the starting gibbsite, indicating that thermal activation resulted in a the small increase in the interlayer distance.

The complete nitrogen adsorption–desorption isotherms of the gibbsite and of the activated alumina samples are shown in Fig. 5. All the isotherms are reversible at low equilibrium pressures, whereas at higher equilibrium pressures, they exhibit a hysteresis loop of the H3 type.[15,16] This type of hysteresis loop indicates the presence of slit-shaped mesopores or pores with narrow necks and wide bodies in the ac-

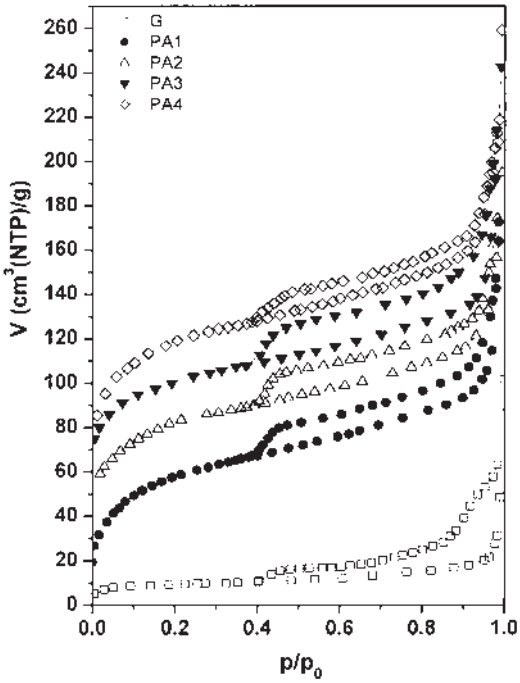

Fig. 5. Nitrogen adsorption–desorption isotherms of the gibbsite (G) and activated alumina samples (PA1–PA4). The ordinate scales are moved up by 20 cm^3(NTP)/g for successive results from PA1 to PA4.

tivated aluminas.[14–16] The entire adsorption isotherm near to $p/p_0 = 1$ are very steep, which is characteristic for the presence of macropores between aggregates.

The values of the specific surface area (S_{BET}), cummulative pore volume (V_p) and diameter of the pores (d_p) of the gibbsite and the activated alumina samples, calculated from isotherms, are given in Table II. As can be seen, upon thermal activation in the temperature range from 883 to 943 K, an increase of the specific surface area up to 250 m^2/g was obtained. In all the activated samples, most of the pores had a diameter between 2.15 and 2.20 nm, which is similar to the diameter of the pores in the starting gibbsite (2.10 nm). However, the pore volumes increased with increasing treatment temperature in the studied range. The probable cause of this behavior of the textural parameters of the activated aluminas was the rapid evaporation of the water in the gibbsite which came from inside the grains to the surface under great pressure. Taking into account that the sizes of the gibbsite crystals were between 100 and 1000 nm,[17] the size of the developed pores indicates that they were formed in the interior of the grains of the original crystals.

The surface fractal dimensions, D_f, of the particles were obtained from the low p/p_0 region of the N_2 adsorption isotherms using a modified Frenkel–Halsey–Hill (FHH) theory. The method is based on the analysis of multilayer adsorption on the fractal surface of the material. Theoretical analysis leads to the expression:

$$\ln\left(\frac{V}{V_m}\right) = C + E\ln\left[\ln\left(\frac{p_0}{p}\right)\right] \quad (1)$$

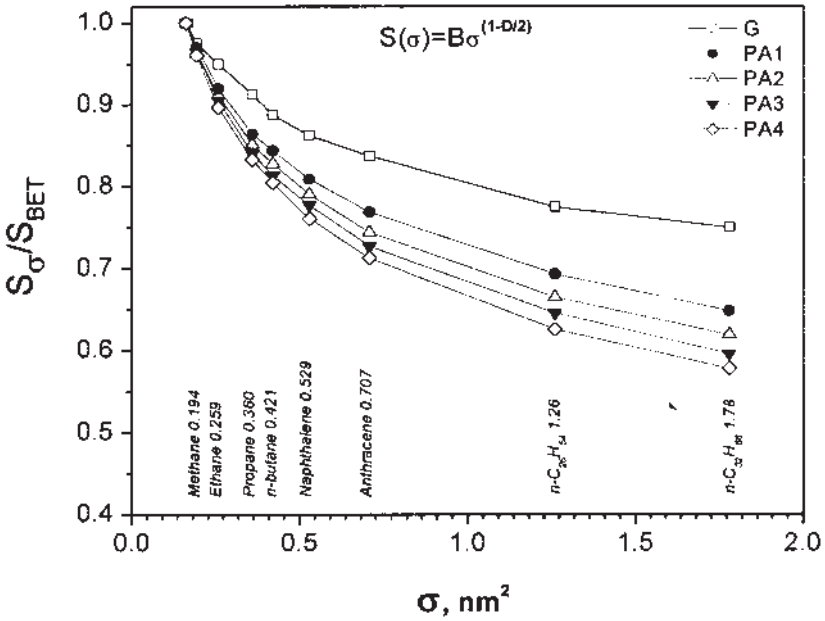

Fig. 6. Effective surfaces of the gibbsite (G) and activated alumina samples (PA1–PA4) in the process of the adsorption of molecules of different size.

where V is the volume of adsorbed gas at equilibrium pressure (p), V_m is the volume of a monolayer of gas and p_0 is the saturation pressure. The constant C is a pre-exponential factor, and E is a power law exponent dependent on D_f, the surface fractal dimension. The appropriate region for obtaining D_f was established through iterative calculation. In every iteration step, the fractal dimension was calculated from the slope of the adsorption isotherms in the appropriate region of the number of layers ($1.0 \pm 0.5 \leq n \leq 2.0 \pm 0.5$), and then new values of n were re-calculated from the obtained D_f. In the present case, only the early stages of the adsorptions gave appropriate values of the fractal dimension ($2 < D_f < 3$). The values of the fractal dimensions obtained using the fractal FHH theory are given in Table II.

TABLE II. Pore structure parameters (S_{BET}, V_p, d_p) and fractal dimension (D_f) of the starting gibbsite and the activated alumina samples

Sample	S_{BET}/m^2 g^{-1}	V_p/cm^3 g^{-1}	d_p/nm	D_f
G	19	0.031	2.10	2.24
PA1	199	0.161	2.15	2.36
PA2	215	0.201	2.20	2.41
PA3	220	0.230	2.19	2.43
PA4	251	0.273	2.20	2.46

The fractal dimension of the surface of the activated alumina samples increased from 2.36 to 2.46, with increasing thermal treatment temperature, indicat-

ing that the surface irregularities of the activated aluminas were greater than those of the starting gibbsite (fractal dimension 2.24).

The values of the fractal dimension (D_f) of the alumina samples and their specific surface area (S_{BET}) were used to calculate the surface accessible for the adsorption of molecules of know molecular cross-section area $S(\sigma)$. These calculations were performed using the fractal equation:

$$S(\sigma) = B\sigma^{(1-D_f/2)} \quad (2)$$

as well as literature data[11] for the cross-section area, σ, of the adsorbates. The dependence of $S(\sigma)/S_{BET}$, *i.e.,* the effective surface, for all the alumina samples on the cross-section area of the adsorbate (σ) is shown in Fig. 6. As can be seen from this diagram, the effective surface decreased for all samples with increasing cross-section area of the adosrbate molecule. The effective surface decreased the most in the alumina sample having the highest D_f-value, *i.e.*, the alumina obtained at 943 K.

CONCLUSIONS

Activated alumina samples obtained from milled industrial gibbsite after a residence time equal to or longer than 0.73 s had a water content smaller than the stoichiometric water content of alumina monohydrate.

The X-ray diffractograms of all the activated samples showed only two major diffraction peaks, corresponding to crystalline gibbsite. The intensity of the gibbsite diffraction lines decreased with increasing temperature, together with slight changes in the other reflections, indicating that the activated alumina samples were either microcrystalline or amorphous.

For all the activated aluminas, the calculated d_{hkl} values were slightly larger than that of the starting gibbsite, indicating that thermal activation led to a small increase of the interlayer distance.

Sorption structural analysis showed that the obtained active alumina samples had slit-shaped pores in the mesoporous range and a specific surface area of 250 m^2/g.

The fractal dimensions of the surface of the starting gibbsite and the activated alumina samples, calculated by applying the FHH method, increased from 2.24 to 2.46 with increasing activation temperature, indicating the occurrence of changes in the texture of the alumina surface during activation.

Knowledge of the fractal dimensions and specific surface areas of the surfaces of the activated alumina samples offers the possibility of estimating, by use of fractal geometry, the effective surface area for the adsorption of molecules with cross-sectional surface areas greater than that of the nitrogen molecule, which is of great importance for the application of these materials in adsorption and catalytic processes.

Acknowledgement: This work was financially supported by the Ministry of Science and Environmental Protection of the Republic of Serbia (Project number TR 6712B and ON 142019).

ИЗВОД

СОРПЦИОНЕ И КРИСТАЛОГРАФСКЕ КАРАКТЕРИСТИКЕ АЛУМИНЕ ДОБИЈЕНЕ У РЕАКТОРУ ЗА ПНЕУМАТСКИ ТРАНСПОРТ ЧЕСТИЦА

ЉИЉАНА РОЖИЋ[1], ТАТЈАНА НОВАКОВИЋ[1], СРЂАН ПЕТРОВИЋ, ЖЕЉКО ЧУПИЋ[1], ЖЕЉКО ГРБАВЧИЋ[2] и АЛЕКСАНДРА РОСИЋ[3]

[1]ИХТМ-Центар за катализу и хемијско инжењерство, Његошева 12, Београд, [2]Технолошко-металуршки факултет, Универзитет у Београду, Карнегијева 4, Београд и [3]Рударско-геолошки факултет, Универзитета у Београду, Ђушина 7, Београд

Кратковременом термичком активацијом гибсита у реактору за пнеуматски транспорт честица на температурама у интервалу од 883 до 943 K и времену боравка од 0.4 до 0.9 s добијен је активни прах алуминијумоксида. Рентгенска структурна анализа показала је да добијени узорци имају висок степен аморфности и мали проценат полазног гибсита. На свим узорцима су одређене адсорпционо–десорпционе изотерме азота из којих је по BET-методи израчуната специфична површина. На основу резултата сорпционо–структурне анализе одређене су фракталне димензије површине FHH-методом, које су послужиле за сагледавање ефективне површине узорака активиране алумине за адсорпцију молекула веће површине попречног пресека од молекула азота.

(Примљено 20. октобра 2005, ревидирано 3. марта 2006)

REFERENCES

1. Yu. K. Vorobiev, B. Badaev, G. Ljubushko, *US Patent* **4 166 100** (1979)
2. U. Bollmann, S. Engels, K. Haupt, J. Kobelke, K. Becker, J. Hille, H.-D. Neubauer, *Z. Chem.* **25** (1985) 273
3. W. Mista, J. Wrzyszcz, *Thermochim. Acta* **331** (1999) 67-72
4. Yu. K. Vorobiev, *USSR Patent* **528733** (1981)
5. Yu. K. Vorobiev, R. A. Shkrabina, E. M. Moroz, V. B. Fenelonov, R. V. Zagrafskaya, T. D. Kambarova, E. A. Levickii, *Kinet. Katal.* ***22*** (1981) 1595
6. L. A. Isupova, Yu. Yu. Tanashev, I. V. Kharina, E. M. Moroz, G. S. Litvak, N. N. Boldyreva, E. A. Paukshtis, E. . Burgina, A. A. Budneva, A. N. Shmakov, N. A. Rudina, V. Yu. Kraglyakov, V. N. Parmon, *Chem. Eng. J.* **107** (2005) 163
7. Lj. Rožić, T. Novaković, N. Jovanović, A. Terlecki-Baričević, Ž. Grbavčić, *J. Serb. Chem. Soc.* **66** (2001) 273
8. K. Malek, M.-O. Coppens, *J. Chem. Phys.* **119** (2002) 2801
9. B. C. Lippens, J. H. de Boer, *Acta Cryst.* **17** (1964) 1312
10. M. J. Watt-Smith, K. J. Edler, S. P. Rigby, *Langmuir* **21** (2005) 2281
11. D. Avnir, D. Farin, *J. Chem. Phys.* **79** (1983) 3566
12. B. C. Lippens, J. H. de Boer, *Acta Cryst.* **17** (1964) 1312
13. H. P. Klug, L. E. Alexander, *X-Ray Diffraction Procedure for Polycrystaline and Amorphous Materials*, 2nd ed., Wiley, New York, 1974, 618
14. S. H. Gregg, K. S. Sing, *Adsorption, Surface Area and Porosity,* Academic Press, New York, 1967
15. B. C. Lipopens, B. G. Linsen, J. H. de Boer, *J. Catal.* **3** (1964) 32
16. K. Sing, D. Evert, R. Haul, L. Moscou, R. Pierotti, J. Rouquerol, T. Siemieniewska, *Pure and Appl. Chem.* **57** (1985) 603
17. P. A. Buyanov, O. P. Krivoruchko, B. P. Zolotovskii, *Izd. Acad. Nauk SSSR, Ser. Khim.* **11** (1986) 39.